CLM-P631

UKAEA

Preprint

CONFINEMENT STUDIES ON A PLASMA GENERATED BY CO_2 LASER IRRADIATION OF ISOLATED D_2 PELLETS WITHIN CLEO STELLARATOR

A. C. WALKER
S. KOGOSHI
T. STAMATAKIS
S. WARD
I. J. SPALDING

CULHAM LABORATORY
Abingdon Oxfordshire

1981

Confinement Studies on a Plasma generated by CO_2 Laser Irradiation of Isolated D_2 Pellets within CLEO Stellarator

ERRATUM

The first sentence of Page 14 should read as follows:-

> The confinement data marginally favour mechanisms (ii) and (iii), since an increase in the toroidal field from B_ϕ = 1T to 1.3T was accompanied by a fall in the observed neutral density by around a factor of 5.

CLM-P631

CONFINEMENT STUDIES ON A PLASMA GENERATED BY CO_2 LASER IRRADIATION OF ISOLATED D_2 PELLETS WITHIN CLEO STELLARATOR

A.C. Walker, S. Kogoshi[†], T. Stamatakis[*], S. Ward and I.J. Spalding

Culham Laboratory, Abingdon, Oxon OX14 3DB
(Euratom/UKAEA Fusion Association)

ABSTRACT

A highly ionised deuterium plasma having an energy content of $\gtrsim$ 370 J has been produced in CLEO Stellarator, using a single CO_2 laser pulse of $\sim$ 2 μs duration. The free-falling deuterium target contained typically 5×10^{18} atoms and was intercepted with a reliability of $\sim$ 40% at fields of 1.3 T. (At zero field the intercept-rate approached 99%). The subsequent trapping efficiency was shown to increase with rotational transform (ι), reaching approximately 50% for $\iota > 0.6$. The energy and particle confinement times of the trapped plasma were both approximately 0.6-1.4ms. This containment is several orders of magnitude less than the neoclassical value and $\sim 1/5$ of that in subsequent ohmically-heated afterglow and microwave-heating experiments. (The latter, however, produced rather higher electron temperatures than the peak value of $T_e \sim 28$ eV observed here). The rapid energy-loss is attributed to charge-exchange on a localised neutral background having a measured density of $\lesssim 5 \times 10^{16}$ m^{-3} (corresponding to < 1% of the injected pellet inventory). Means for reducing the charge-exchange losses and wall-recycling in subsequent work are suggested.

[†]Permanent address: Department of Electrical Engineering, University of Tokyo, Japan.

*Attached from Royal Holloway College, University of London.

(Submitted for publication in J. Phys. D., Appl. Phys.)

JANUARY 1981

1. INTRODUCTION

The Stellarator confinement concept utilises magnetic fields wholly generated by external conductors. For this reason it is unnecessary to deliberately induce currents within the confined plasma, thus facilitating the conceptual design of a steady-state fusion reactor. Experimental studies on the CLEO Stellarator (Atkinson et al 1977) had indicated that with low induced toroidal currents the energy confinement appeared to improve significantly. For these two reasons various techniques have been developed for generating energetic plasmas within CLEO Stellarator without the use of a continuous electrical discharge (Atkinson et al 1979).

Three approaches have been investigated as part of the CLEO programme:

(i) sustainment of a discharge-generated plasma by neutral beam injection;
(ii) generation and heating of the plasma by microwave radiation, and
(iii) generation of a hot plasma by laser-irradiation of a D_2 target located at the centre of the confinement volume.

The latter technique is described in this paper. It contrasts with the microwave approach mainly in that the shorter wavelength (visible or infra-red) laser radiation needs a much higher plasma density ($\gtrsim 10^{25}$ m^{-3}) for significant coupling to occur, from which follows the necessity of using solid, in this case frozen deuterium, targets.

The earliest work on the laser filling of magnetic traps was carried out using ruby lasers and magnetic mirror or cusp confinement configurations. Linlor (1964) described results using extended Au and Al targets for the plasma source. Other groups used electrodynamically suspended, 10-100 μm diameter particles of Al (Sucov et al 1966) or LiH (Haught et al 1969, Lubin et al 1969, Haught et al 1970) as the laser target. More recently the work with LiH particles was extended to higher energy, using a 40 Joule, Nd:Glass laser for the Laser Initiated Target Experiment (LITE), where $\sim 10^{17}$ ions ($\sim 10^{19}$ m^{-3}) with energies of $\sim$ 400 eV ($T_e \sim$ 10 eV) were generated within a minimum-B mirror machine before subsequent neutral beam injection (Haught et al 1978). Low z, hydrogenic plasmas have also been produced within cusp configurations by irradiating freely falling solid deuterium pellets with Nd:Glass lasers (Kitzunezaki et al 1974, Pechacek et al 1980).

The first experiments on laser-plasma filling of toroidal traps were performed on the TOR-I (Andryukhina et al 1971) and PROTO/CLEO (Bolton

et al 1971) stellarators. In the latter experiment a 15 Joule Nd:Glass laser was focused onto Li or Be wires positioned just outside the separatrix. Electron and ion temperatures of 2-3 eV were achieved at densities of up to 10^{19} m^{-3}. The three main disadvantages of that technique were the extended nature of the target, which inevitably results in neutral vapour being produced from around the plasma generation area; the $z \geq 3$ plasma produced by the metal ions and the need for the plasma to penetrate into the magnetic trap. These problems are avoided by using isolated pellets of solid deuterium irradiated near the toroidal axis. Such an experiment, using a Nd:Glass laser on the WIIb stellarator, has been described by Baumhacker et al (1977, 1980). They generated densities of up to 8×10^{18} m^{-3}, with an estimated electron temperature of somewhere below 5 eV. CLEO is approximately ten times the volume of these earlier stellarators and therefore required more ions and greater laser energy to achieve the same density and temperature. The work described here is therefore unusual in two respects:

(i) trapped deuterium plasma having densities exceeding 10^{19} m^{-3} and electron temperatures greater than 10 eV have been produced by the laser-plasma method within a large stellarator, and

(ii) the source used for generating this plasma was a single-pulse kilojoule CO_2 laser.

A cold-cathode electron-beam controlled CO_2 laser was preferred over a solid state laser for the following reasons:

(i) It is electrically efficient (10 ∿ 20%) and is scalable to very high energies over a wide choice of pulse-durations (∿ 10^{-9} to 10^{-4} s).

(ii) Heating occurs at a (critical) density $\lesssim 10^{-2}$ of that produced by Nd or ruby and other visible lasers, so that subsequent volume expansion and three-body recombination is weaker.

To match the plasma energy inventory appropriate to ohmic heating in CLEO, say 400 J for a plasma density and temperature of $n_e = 2.5 \times 10^{19}$ m^{-3} $T_e = 200$ eV respectively, an incident laser pulse of $\gtrsim 1$ kJ was specified to allow for heating and probable trapping losses of the expanding laser-plasma (Spalding et al 1976). The work presented here represents the outcome of an initial experiment intended to demonstrate technical feasibility, rather than detailed optimisation of CLEO confinement parameters. Of particular interest are novel results on the plasma trapping efficiency, and possible means for improving the subsequent energy confinement.

2. EXPERIMENTAL APPARATUS

The l = 3 CLEO Stellarator (Reynolds et al 1974), the CO_2 TROJAN laser (Reynolds et al 1980), and the cryogenic deuterium-pellet source (Kogoshi et al 1980) have each been described elsewhere. We shall here summarise how they were integrated for the present experiments.

2.1 TROJAN CO_2 Laser

TROJAN is a single-module, electron-beam controlled, pulsed-discharge CO_2 laser employing a commercial (Systems, Science and Software) electron gun. The active volume is 0.2 x 0.25 x 2 metres and it can be operated at laser gas pressures of up to 2 atmospheres. The Culham-built DC charged sustainer-bank has a maximum stored energy of 62.5 kJ at 200 kV. For the present work it was filled with a gas mixture of 2:1, CO_2:N_2 at a pressure of 1 standard atmosphere. A sustainer field of 700 kV/m (140 kV) permitted operation with an efficiency (laser output to total electrical input) of $\sim$ 11%. The system was operated as a simple oscillator, with an unstable confocal mirror resonator having a magnification of 2.6. The output was an unpolarised, rectangular (annular) beam of external dimension 0.17 x 0.19 m, having an energy of $\sim$ 1.5 kJ. The pulse consisted of an initial, 50-80 ns duration, gain-switched spike having a mean peak-power of 5-8 GW, followed immediately by a tail of $\sim$ 1 GW mean power lasting about 2 μs.

2.2 Deuterium Pellet Production

The prototype deuterium pellet-source was developed at IPP, Garching (Baumhacker et al 1976) as part of the WIIb-stellarator laser-filling experiment (Baumhacker et al 1977). Collaboration between Garching and Culham resulted in the design of a miniaturised version, manufactured by Leybold Heraeus, suitable for the more restricted access and different irradiation geometry used on CLEO. The device, a continuous flow liquid helium cryostat, is shown schematically (Figure 1). Deuterium gas is condensed, compressed at a pressure of 250 atm, and a 300 μm diameter cylindrical stick is then extruded through a nozzle at the bottom. Two heated wires cut off a pre-set length of the D_2, which drops freely under gravity to the laser focus. A typical pellet is shown in Figure 2. Various lengths between 600-900 μm were used, giving (4-6) x 10^{18} deuterium atoms per pellet.

The size of each pellet was estimated from a TV video recording of its projected image, just before it detached (see Figure 2a). By measuring

the pressure rise when pellets were dropped into a known volume, it was shown that the deuterium density agreed within a 16% experimental accuracy, with the published value of 6×10^{28} atoms m^{-3} at 12K. Assuming this value for the density, the particle number for any specific pellet could subsequently be estimated to ± 15%.

The arrival of the pellet at the laser focal point was detected by the interruption of a low power He-Ne laser beam used to align TROJAN and the focusing system and which corresponded accurately to the main laser output. The focal region was imaged (one to one) onto a detector so that the He-Ne laser focus lined up with a 0.25 mm radius aperture placed in front of it. This aperture acted as an external reference for the pellet trajectory and defined a 0.5 mm area within which the pellet had to fall for TROJAN to be fired. Variation of the pellet position within this area and, more importantly, random tumbling of the (non-spherical) pellets resulted in some shot to shot variations in the parameters of the plasma generated.

Improvements in operating procedure and some modifications to the equipment (Kogoshi et al 1980) permitted a pellet detection rate of > 99% after a fall of 0.3 m into the un-energised CLEO Stellarator. This intercept rate was achieved without active control of the pellet trajectory or the laser-focus, and relied on careful temperature-control during the pellet production cycle. Movements due to incomplete mechanical decoupling from the torus of the pellet-source and the focusing and pellet detection optics decreased the probability of a pellet falling with the required spatial accuracy to 75% when the toroidal field coils were energised.

Synchronisation of the pellet's fall with the 4 second toroidal-field pulse was achieved by phasing the pellet production and CLEO charging cycles. The helical (stellarator) winding on CLEO is energised for a much shorter period (0.25s) and to ensure accurate timing was triggered by the pellet itself as the latter left the cryostat. Machine safety limited the time available for triggering to a 0.5 sec interval. As a result jitter in the pellet fall-time, a consequence of the careful (slow) cutting necessary for spatial accuracy, gave a synchronisation probability of $\sim$ 50%.

These spatial and temporal accuracies were quite adequate for initial

experiments permitting ∿ 100 pellets to be irradiated within CLEO. For the method to become a routine plasma production technique further improvement of the mechanical isolation (or possibly pellet or laser-focus steering) should permit the reliability to approach 100%.

2.3 Laser Beam Transport and Focusing System

CLEO Stellarator is positioned on a platform above, and to one side of, the TROJAN CO_2 laser; Figure 3 shows the overall layout. The laser output was guided ∿ 18 metres to the focusing optics by three 0.3 m diameter metal mirrors. The geometry of the focusing system is shown schematically in Figure 4 along with the laser and a target chamber used for the preliminary experiments. The 4.5 m focal length focusing mirror had an effective f-number of f/22, the lowest value compatible with producing a focus beneath the pellet-dropper position and remaining within the available input-port dimensions. The resultant focal irradiance distribution was shown to be close to diffraction limited, having a FWHM diameter of 300 μm with 80% of the energy within a 1.5 mm diameter spot. At the peak of the pulse the irradiance averaged over the pellet dimensions is ∿ 6×10^{15} W m^{-2}, reaching a central maximum of 1.8×10^{16} W m^{-2}.

The focusing system was mounted on a port looking approximately tangentially along the toroidal axis, and opposing a similar port occupied by the pellet detection optics. The angle between the laser and the toroidal axis at the point of pellet irradiation was ∿ 30°.

3. THE LASER-GENERATED PLASMA

The target-chamber of Figure 4 was used for simulating the irradiation geometry in CLEO, whenever measurements were required of laser-plasma generation in the absence of magnetic fields. This arrangement provided good access for the following diagnostics:

(i) IR detectors to determine the absorption of the 10μm laser pulse;
(ii) ruby laser shadowgraphy and interferometry to assess the degree of pellet vaporisation and ionisation;
(iii) Faraday-cup charge collectors to determine the numbers and energy of the ions in the expanding plasma, and
(iv) calorimetry to measure the total particle/radiation flux resulting from the pellet irradiation, and to check the overall energy balance.

3.1 Absorption of Incident 10 μm Radiation

Figure 4 shows the location of the detectors used to measure incident and reflected power (P1,P2) and energy (E1,E2). In addition burn-film techniques (Walker et al 1978a), together with additional infra-red detectors, were used to measure the refracted and scattered energy. The losses measured by these techniques amounted to (19 ± 13%) of the incident energy of ∿ 1.3 kJ (Walker et al 1978b). Energy transmitted past the pellet during the early phase of irradiation (before the plasma has time to fill the focal volume) falls within the solid angle reserved for the pellet detection optics and is therefore not measured in this experiment; however, refraction calculations suggest a further loss of ∿ 15% due to this factor.

3.2 Pellet Ionisation

Shadowgraphs of the pellet and plasma during and just after irradiation indicated virtually complete vaporisation of the pellet for incident pulse energies of $\gtrsim$ 1.3 kJ (Walker et al 1978b). Semi-quantitative measurements of the level of ionisation were obtained with double-pulse, single wavelength, holographic interferometry (Gatenby and Walker 1979). Figure 5 shows representative interferograms taken at different times during a series of irradiation pulses. The maximum number of detectable electrons in any one interferogram corresponds to ∿ 10% of the pellet. However, this must be an under-estimate of the percentage ionisation because the duration of the laser-pulse is so long (2 μs) that ablating plasma passes from the field of view and reaches the wall of the target chamber before the end of the pulse. Noting the observed plasma expansion-velocities of between 2 and 8 x 10^5 m/s, the measured fringe-shifts are in fact entirely consistent with a total ionisation of $\gtrsim$ 50%. This agrees with the observation that the maximum amount of neutral material positively identifiable in the interferograms amounted to only ∿ 2% of the initial pellet (cf. Figure 5d). However, with this single-wavelength (λ = 0.69 μm) measurement the sensitivity to neutrals is low, being approximately 2% of that for free electrons. These measurements therefore indicate that the pellet ionisation lies between 50 and ∿ 98%.

Limited information on the ionisation of the pellet was also obtained from the Faraday-cups. These consisted of fully-enclosed earthed chambers with a ∿ 0.4 mm diameter pinhole facing the plasma. Within each enclosure was an isolated collecting cup, biased negatively to repel the electrons.

The signals obtained were independent of the voltage magnitude above 40 V; typically - 67 V was used. The signals also scaled as expected (i.e. roughly as $1/r^2$) with distance from the plasma source. Despite these checks it became apparent from the measurements discussed below that the charge collectors underestimated the true ion-flux emanating from the pellet. Four or five of the cups were used to detect plasma expanding at angles relative to the incident laser-beam of 0° (i.e. directly back towards the laser), 45°, 90° and 175°. The angular distribution of the detected plasma is shown, averaged over 16 shots, in Figure 6(a).

The total ion emission was estimated from measurements of this type by integration over the expansion geometry. Figure 7(a) illustrates how the total number of ions appeared to vary with laser-pulse duration. By increasing the duration of the electron beam, the laser output could be extended from a $\sim$ 0.3 μs pulse containing $\sim$ 450 J to one lasting $\sim$ 2.1 μs with $\sim$ 1.4 kJ energy. Despite a threefold increase in incident energy, the average number of ions detected increased by only 60%, to some 10 $\sim$ 20% of the pellet inventory; the integrated ion energy similarly appeared to be insensitive to pulse duration (Figure 7(b)). Neither of these observations is consistent with the interferometric measurements discussed above which showed a continuing interaction during the later part of the longer pulse, nor with the calorimetric and plasma-confinement data described below. The cause of this discrepancy, discussed more fully in §3.3 is believed to be a build up of cold neutral material near the target chamber walls which results in charge-exchange neutralization of the expanding ions arriving later in the irradiation. Indeed, calculation indicate that the degree of pellet ionization inferred from the Faraday-cup signals (10 - 20%), must be an underestimate, and again a total ionization of $\gtrsim$ 50% is estimated.

3.3 Plasma Energy

Time of flight velocity measurements of those ions detected by the Faraday-cups permitted the measurement of individual ion energies and the angular distribution of the energy they carried. The most energetic ions were observed expanding directly towards the incoming laser beam (i.e. 0°) at velocities corresponding to 8 keV deuterons. Such ions were few in number and carried only a small fraction of the total energy. Even so, the total energy flux also peaked along the line of the incoming radiation, as shown in Figure 6(b). The average ion kinetic-energy for the full 4π expansion was measured to be $\sim$ 300 eV when using the full ($\sim$2 μs) laser

pulse. Within the initial $\sim$ 0.2 μs portion of the pulse an average energy per particle of $\sim$ 500 eV was observed - in good agreement with the maximum electron temperature for dense plasma near the critical density of 100 - 200 eV (deduced from x-ray emission analysis by metal foil absorbers)(Kler 1980). The total of $\lesssim$ 50 J integrated plasma energy determined with the Faraday-cups in this manner is clearly an underestimate, for the reason discussed earlier (e.g. see Figure 7(b)).

To provide a more accurate measure of the energy carried by the plasma, a carbon-cone calorimeter was therefore used in conjunction with a deflecting magnetic field (Figure 8). McCracken and Stott (1979) describe results showing that deuterium ions of energy 10 eV to 1 keV striking a carbon surface are absorbed with efficiencies of 50 to 90% respectively; moreover, those particles reflected carry only 30-50% of their initial energy and are predominantly neutral. It follows that for $\sim$ 300 eV deuterons over 90% of the incident energy should be absorbed, with the calorimeter geometry illustrated. Two calibration tests were performed using, for convenience, large-area polythethylene sheets rather than falling pellets as a laser target. Firstly, it was demonstrated that the 0.25 T magnetic deflection field successfully reduced the signal from a time-integrating charge-collector, of the same aperture and position as the calorimeter, to only 13% of that recorded without the field. Secondly, the calorimeter itself was tested with no deflection field; viewing the plasma at 45° from the laser beam. After scanning over the 2π solid-angle (using Faraday-cup results to give the relative energy distribution) it was shown that the signal corresponded to a total energy that, on average, matched the laser energy of $\sim$ 1.5 kJ to within 10%. Furthermore, the signal was found to scale linearly with the total incident laser energy. A final check with the deflection field at 0.25 T demonstrated, for this test plasma, that 75% of the energy reaching the calorimeter resided in charged particles.

Using D_2 pellet targets and an incident laser energy of $\sim$ 1.5 kJ it was deduced from the calorimeter signals and the distribution of Figure 6(b)) that the average for the total energy into 4π steradians was 410 J. When the field was increased from zero to 0.25 T this total was reduced to an average value of 225 J. Making a small correction ($\sim$ 13%) for ions penetrating the field, it follows that $\sim$ 210 J of the detected energy was carried by charged particles.

To assess the contribution due to scattered laser radiation a thin polyethylene film (70% transmitting at 10 μm) was placed over the calorimeter. In agreement with the results described in §3.1, it was found that only 10% of the total signal could be ascribed to scattering. The possibility of x-ray emission being a significant factor in the overall energy balance was also investigated but it was shown from absolute photographic measurements that this corresponded to < 2 J, in agreement with calculation.

It therefore seems very probable that the remaining energy is carried by fast neutrals generated by charge-exchange collisions. Ionization of neutrals ablating from the pellet should occur rapidly under these high density coronal conditions (cf. Appendix) and the initial target-chamber pressure of $< 10^{-5}$ Torr was too low to give significant charge-exchange effects. However, our measurements have shown that the first 80 ns portion of the laser pulse causes $\gtrsim 10^{18}$ ions/m^2 to impinge upon the target chamber wall, at 45° from the laser. Approximately 20% of such ions are predicted to be reflected as neutral atoms, while the rest should desorb 1 ∿ 10 molecules per ion from the unbaked surface (McCracken and Stott 1979). The resulting neutral density is therefore such that up to ∿ 90% of the ions arriving subsequently would make charge exchange collisions. This explanation resolves the discrepancy between the energy deduced from the Faraday-cup signals and the calorimeter measurement of charged particle energy, in that diffusion of neutrals having an energy of typically 5 eV across the 0.4 mm diameter pinhole takes only ∿ 30 ns, while the time taken to 'close' the 18 mm calorimeter aperture is over a microsecond. More importantly, given efficient trapping of the plasma by the CLEO magnetic fields, the full 370 J carried by the expanding plasma would remain in ionized particles.

3.4 Summary of Energy Balance

For an incident 2 μs laser pulse of 1.5 ± 0.15 kJ, the energy-balance, averaged over ∿ 30 measurements on D_2 pellet falling into the ungettered and unbaked target-chamber, and the estimated errors of measurement, are summarised in Table 1.

Table 1 - Energy Balance

Item		Mean (J)	Error (J)
1.	Plasma Energy	370	± 150
2.	Re-radiation	$\lesssim$ 2	small
3.	Dissociation and ionization	15	-
4.	Refraction/scattering	285	± 195
5.	Direct transmission loss (around the pellet)	$\sim$225	± 115
6.	Apparent energy deficit	603	± 610

NB - 1. Calorimeter measurement: ions + neutrals
2. X-ray flux measurement/calculation
3. Calculated
4. Burn-film and λ = 10 μm detector measurements
5. Estimated from interferometric measurements, using ray-tracing calculations, cf. Walker et al 1978 a and b.

As can be seen there are large cumulative errors, in the energy balance, arising from integration of the data over the 4π geometry. The major problem is the determination of the effects of charge-exchange (and possibly electron-thermal conduction) on the apparent energy distribution of the plasma. In our view the re-radiation and 10 μm measurements (2 and 4) are completely reliable, but the estimate of the loss arising from transmission straight past the pellet is more difficult. (However, our estimate is fully consistent with direct measurements on similar stationary, $(CH_2)_n$ targets). In summary, taking the extremes of the above quoted errors the energy budget can be balanced. This suggests that the total energy carried by the expanding plasma is more likely to be greater than 370 J rather than less, i.e. that the heating efficiency for the (randomly) tumbling pellets is greater than 25%. (Higher average efficiencies should be achievable by steering either the pellet or the laser beam to ensure optimum alignment for every shot).

4. CONFINEMENT RESULTS

The laser-generated plasmas discussed in the previous sections were successfully generated, under similar irradiation conditions, within the CLEO Stellarator. Measurements were made of the trapped densities, temperatures and the particle and energy loss rates.

4.1 Peak Densities

Average line-of-sight density measurements were made using a 2 mm wavelength microwave interferometer, 105 degrees around the torus from the plasma generation point. No measurement of the density radial profile was attempted. It is assumed that it was similar to that obtained within PROTO-CLEO with current-less plasmas (Lees 1974) and that it can be approximated by a flat profile out to $^2/_3$ of the effective radius, falling to zero at full radius. This effective radius is only a weak function of the rotational transform, ι, and can be given an average value of 0.1 m. With these assumptions a central density is deduced.

Figure 9(a) shows a typical density/time plot, in this instance for one of the high density shots. The initial rapid rise is followed by a $\sim$ 250 μs period when the density is a maximum, finally decaying on the time-scale of a few milliseconds. The peak density observed was found to be a function of the ratio of the currents in the toroidal-field coils and the helical winding, i.e. the rotational transform. This can be seen in Figure 10 where, despite the considerable statistical scatter of results, the average peak density for values of ι (at the limiter) of > 0.6 is 5 times that for $\iota = 0$ (i.e. toroidal field only). Further evidence of poor trapping in the absence of a rotational transform came from time-of-flight measurements (described further in section 4.3) which showed considerably delayed plasma arrival times for $\iota = 0$, corresponding to ion energies $\sim$ 24 times lower than for high ι, thus implying strong wall interactions. These results contrast with those of Baumhacker et al (1977), in the WIIb stellarator, where laser-plasma capture was described as only weakly dependent on rotational transform.

The maximum central density observed was $3(+\ 2, -\ 0.5) \times 10^{19}\ m^{-3}$, corresponding to 50(+ 40, - 27)% of the pellet (allowing for uncertainties in both pellet size and the profile). The absolute value of the magnetic field was not varied sufficiently (at constant ι) to give a clear indication of the dependence of trapped density upon field strength. The results described here were made with a toroidal field, $B_\phi = 1.3T$. (It was observed that with zero fields the (slow) microwave interferometer signal was only marginally smaller than in the $B_\phi = 1.3T$, $\iota = 0$ case).

4.2 Particle Confinement Time

The final density decay is unaffected by ionization processes due to the low electron temperature and neutral density observed at this time. Thus the particle confinement time, τ_p, can be obtained directly from the slope of the semi-log density plot. Figure 9(a) shows τ_p to be about 1.3 ms after $\sim$ 3 ms. At earlier times, when ionization rates are significant and must be taken into account, shorter confinement times of around 0.6 ms are deduced. The average value for the final decay time-constant at maximum ι was 1.4 $\pm$ 0.4 ms. This is not significantly different from the τ_p with no rotational transform, which was measured as 1.0 $\pm$ 0.4 ms. Thus, although the full stellarator fields certainly improved the initial trapping of the plasma, the subsequent confinement was not particularly sensitive to the rotational transform.

4.3 Trapped Energy

Information on the plasma energy was derived from the density rise-time observed on the microwave interferometer and on a Langmuir probe (165^{o} from the plasma generation point). The time between the laser shot and the density rising to half its peak value was typically $\sim$ 5-10 μs (see, for example, Figure 9(b)). This corresponds to ion energies, assuming direct flight round the torus, of $\sim$ 600 eV in good agreement with the average ion energies produced by the initial laser pulse spike, discussed in section 3. A more detailed analysis of the density rise permits the deduction of the total energy carried by the ions which reaches the opposite side of the torus. Comparing the Langmuir probe signal obtained near the torus centre and near the edge, the plasma was shown to arrive over the full confinement volume (at 165^{o} from the source) and the profile used for the peak density was again assumed to be appropriate. Only low density shots were analysed in this way (i.e. peak densities 4-7 x 10^{18} m^{-3} with ι - limiter = 0.48) due to the microwave density diagnostic being unable to follow the very rapid rise to the higher densities. It was found, for these shots, that the ions carried a total kinetic energy of $\lesssim$ 50 J. If the same average energy per ion ($\sim$ 500 eV) is assumed for the higher density (high ι) shots, this implies that up to 215 J energy was initially trapped as circulating ions. It also implies that, given the total initial particle energy of $\sim$ 370 J discussed in §3.3, $\sim$ 75% of the pellet must have been ionized in these shots and that up to 60% of the plasma energy was trapped by the stellarator fields in the first stages of the filling process.

4.4 Energy Confinement Time

Other than the initial time-of-flight measurements described above, the ion energy (or temperature) was not monitored. The electron temperature was measured by (ruby laser) Thomson scattering, and with a Langmuir probe. The latter was operated with a 40 V sweep and gave reliable measurements of T_e up to 10 eV. Synchronisation difficulties permitted only a limited number of Thomson scattering results, giving a maximum recorded temperature (measured during the first 0.5 ms) of $T_e = 28 \pm 5$ eV at a density of $n_e = 1.7 \times 10^{19}$ m^{-3}. Four measurements were made using the Langmuir probe during each shot; these showed $T_e \sim 10$ eV after ~ 2 ms, as shown in Figure 9(a). The time constant for the temperature decay after 1 ms was found to be comparable to the particle confinement time of 1-2 ms. In the absence of rotational transform the low density plasma had an electron temperature typically a factor of 5 smaller. Thus, as with the particle trapping, the rotational transform improved the initial energy trapping but not its longer term confinement.

4.5 Neutral Density Measurements

The neutral density in the confined plasma is important because it determines the rate at which ions lose their energy through charge-exchange. The base pressure in CLEO before a shot was typically 6×10^{-8} Torr, while $\sim 75\%$ of the torus wall was gettered with titanium to minimise gas desorption from its surface. Neutral-densities were deduced from H_α emission in three regions: near the pellet irradiation point (0^o), near the limiter (135^o) and at 165^o round the torus. Just after the laser shot the neutral density, averaged across the torus cross-section, was $\sim 5 \times 10^{16}$ m^{-3} close to the irradiation point and about ten times less at the other positions. After about 1 ms these values converged to a uniform neutral density value of $\sim 1 \times 10^{16}$ m^{-3}. Averaging around the torus the maximum number of neutrals measured in the confinement volume is $\sim 7 \times 10^{15}$, corresponding to an averaged density of 2×10^{16} m^{-3}. This represents only 0.1% of the original D_2 pellet but is sufficient to cause rapid charge-exchange losses. There are four possible mechanisms for producing these neutrals:

(i) incomplete pellet ionisation, with only partial trapping of the cold deuterium atoms on the (gettered) walls;

(ii) reflection of non-trapped D^+ ions from the torus walls as neutrals;

(iii) desorption of surface gases from the walls by the non-trapped plasma.

(iv) desorption of surface gases from the walls by the scattered laser radiation.

The confinement data marginally favour mechanisms (ii) and (iii) since an increase in the toroidal field from B_ϕ = 1.3T was accompanied by a fall in the observed neutral density by around a factor 5. Mechanism (iii) also appears the most likely on the basis of calculations summarized in the appendix.

5. DISCUSSION

The equipartition-time in the ablating $n_e \sim 10^{25}$ m^{-3}, T_e = 100-200 eV, corona surrounding the pellet is less than 10 ns, and T_e and T_i remain closely coupled during a subsequent expansion which transfers much of the absorbed energy to directed motion of the ions. The expansion is neither fully adiabatic, in the sense discussed by Dawson (1964) and Crowe et al (1975), nor fully isothermal - because of the finite duration of the laser heating pulse. Before the end of the 2 μs laser pulse the density of the expanding plasma has fallen to such a value ($\sim 4 \times 10^{21}$ m^{-3}) that the momentum of the 500 eV deuterons is balanced by the pressure exerted by the 1.3T stellarator field (i.e. $\beta = 1$). The plasma is subsequently trapped and starts to expand along $\underline{B}$, as illustrated in the framing-camera photographs of figure 11. (Note also the longer duration of the visible radiation in the 1.3 T field, indicating a higher electron density due to the radial confinement). The plasma radius at this stage is around 10-20 mm and the electron temperature can be estimated as $\sim$ 50 eV (based on an irradiance to the one-third power, T_e scaling). This gives a resistivity of $\sim 2 \times 10^{-3}$ ohm-mm and hence a (classical) field relaxation time of $\sim$ 50 μs - consistent with apparent gross confinement during the (few μs) time-scale of the initial plasma expansion. After termination of the laser pulse further expansion along $\underline{B}$ results in adiabatic cooling and an approximately ten-fold increase in resistivity. The magnetic field can then penetrate the plasma column, relaxing to nearly the vacuum configuration. As the plasma continues its expansion, filling the confinement region, the classical cross-field diffusion rate falls due to both the gentler density gradient and the rise in T_e caused by the diffusion process itself. Only at this stage can the plasma be said to be trapped.

The improvement in trapping efficiency which occurs as the rotational transform is increased (Figure 10) is a novel result, and could be due to shear-stabilisation of Rayleigh-Taylor instabilities during the $\beta \lesssim 1$ deceleration phase. Alternatively it may be significant that the trapping improves at a value of ι which brings the magnetic separatrix inside the

limiter, thus reducing external contact with the confinement volume.

5.1 Particle Confinement

The ratio of the connection length to the electron mean-free path is $\gtrsim 1$ for the laser-plasmas discussed in § 4, so that the appropriate neoclassical particle confinement-time, discussed by Pfirsch and Schluter (1962), is given by

$$\tau_{ps} = \frac{4.28 \times 10^{13}\ a^2\ T_e^{\frac{1}{2}}\ B^2}{n\ell n\Lambda\,(1 + T_i/T_e)(1 + \iota^2)} \qquad (1)$$

where a is the minor radius, $\ell n\Lambda$ is the Coulomb logarithm and the units are expressed in metres, eV, Gauss and seconds. Lees (1974) had found this theory to give good agreement with the early (high z) laser-plasma experiments on PROTO-CLEO. Assuming $n = 2 \times 10^{19}\ m^{-3}$, $T_e = 20eV$, $T_i \lesssim 500eV$ at peak density, and $n = 2 \times 10^{18}\ m^{-3}$, $T_e = T_i \sim 2eV$ subsequently, the observed confinement in CLEO is respectively $\sim 3 \times 10^{-2}$ to 10^{-3} of the neoclassical value τ_{ps}; indeed it more closely approaches the Bohm time

$$\tau_B = 2.7 \times 10^{-4}\ a^2\ B/T_e\ . \qquad (2)$$

The source of the enhanced diffusion has not been determined: note that poor electrical connection around the torus, or alternatively orbit-changing charge-exchange collisions, could contribute initially.

5.2 Energy Confinement

The thermalisation-time for 500 eV (directional) ions to lose 50% of their energy to a $T_e = T_i \sim 20$ eV background plasma is ~ 0.6 ms, comparable to the particle confinement-time. Complete thermalisation of the trapped energy would have given $T_e = T_i = 150 \sim 200$ eV. Thus the observed fall of T_e from $\sim 30eV$ to ~ 2 eV within the first 2 ms can only be explained by postulating a very rapid loss of ion-energy. In fact, the time constant for 50 eV-1 keV deuterons to charge-exchange with atomic deuterium is 0.7-1.7 ms, at the measured value of $n_o = 2 \times 10^{16}\ m^{-3}$. The probability for re-ionization of an atom excaping with an energy of 500 eV from the centre of the plasma is only $\sim 8\%$ at the peak densities achieved. Thus Ti (and hence T_e) is expected to decay on the millisecond time-scale observed.

6. CONCLUSIONS

A major objective of this initial experiment: to establish the feasibility of filling CLEO with a laser generated plasma, was demonstrated with a pellet intercept-rate of 40% at the toroidal field level of 1.3 T. The means identified for improving this reliability in any subsequent experiment, were further (bellows) isolation of the pellet-dropper from mechanical vibration of the torus and lengthening the period within which the helical field could be pulsed.

A single λ = 10 μm pulse of 1.5 kJ proved sufficient to highly-ionize the free-falling cryogenic pellet, generating $\lesssim 4.5 \times 10^{18}$ deuterium ions. Between 10% and 40% of the incident energy was absorbed in the low z plasma and $\lesssim$ 60% of this plasma energy, and of the injected atoms, were subsequently trapped in CLEO. The trapped plasma (free of macroscopic toroidal current) experienced a high particle loss-rate of uncertain origin and a rapid energy-loss due to charge-exchange on a localised neutral background having a measured density of $\lesssim 5 \times 10^{16}$ m^{-3}. The resulting plasma life-time, of a few ms, was a factor of $\sim$ 5 shorter than that obtained in subsequent ohmic-heating after-glow and electron-cyclotron-heating experiments on CLEO which had, however, a slightly higher electron temperature and lower T_i/T_e ratios (cf. Atkinson et al 1979).

Some relatively minor changes to the trapped plasma parameters would reduce the charge-exchange losses: in particular, a modest increase in the trapped electron density and electron temperature. As a specific example, an increase of these parameters to 10^{20} m^{-3} and 100 eV respectively would reduce the probability of a 500 eV deuterium atom escaping from the centre of the torus without re-ionisation to $\lesssim$ 20% and of a 100 eV atom to $\lesssim$ 3%. Thus the direct energy loss and the wall recycling should both be decreased very significantly. It should prove possible to increase the trapped particle density by irradiating larger-diameter pellets with a longer-duration laser pulse. In particular, a 1 mm diameter pellet 1 mm long would contain $\sim 5 \times 10^{19}$ atoms and would have the considerable advantage of being more symmetric, thus intercepting more of the laser beam as it tumbled into the focal volume of the laser. This, itself, would increase T_e due to more rapid re-thermalization at higher densities while, additionally, the use of hydrogen rather than deuterium would reduce the equipartition-time by a further factor of 2. Exploratory work at Culham has shown that the cryogenic complication of working with H_2

(rather than D_2) pellets can be overcome with only a modest increase (to $\sim$ 10 ℓ/hr) in liquid helium consumption, and that larger pellets can be readily produced (L.W. Jorgensen, private communication). We conclude that the techniques discussed here should make it possible, assuming equally efficient trapping for the larger pellet, to confine laser-produced plasmas in stellarator geometries under conditions where charge-exchange and wall recycling play a less dominant role. The containment of the resulting plasma would provide an interesting comparison with alternative filling methods, and could lend itself to hybrid experiments, for example, employing simultaneous microwave electron-heating.

ACKNOWLEDGEMENTS

The authors wish to acknowledge the contribution of the CLEO group (in particular, P.C. Johnson), under the direction of D.J. Lees; fruitful collaboration with Dr. M. Salvat's group at IPP; and the interest of Professor T. Sekiguichi and Drs. R.J. Bickerton and D.R. Sweetman in various aspects of this work.

REFERENCES

ANDRYUKHINA E D, BLANKEN R A, VORONOV G S, DONSKAYA N P, RABINOVICH M S, SMIRNOVA A D, FEDYANIN O I, KHOLNOW Yu V and SHPIGEL I S (1971) Lebedev Physics Institute (USSR) Preprint No. 106.

ATKINSON D W, BARTLETT D, BRADLEY J, DELLIS A N, HAMBERGER S M, LISTER J B, LEES D J, MILLAR W, SHARP L E, SHATFORD P A (1977), Proc. 8th Europ. Conf. on Controlled Fusion and Plasma Physics, Prague, Vol. II pp.93-107 (Culham Report CLM-P505).

ATKINSON D W et al (1979), Proc. 9th Europ. Conf. on Controlled Fusion and Plasma Physics, Oxford, Paper A2.6 (Culham Laboratory, Abingdon, UK).

BAUMHACKER H, BRINKSCHULTE H, LANG R S and RIEDMULLER W (1976), Proc. 9th Symp. on Fusion Technology (Pergammon Press) 873.

BAUMHACKER H, BRINKSCHULTE H, RIEDMULLER W, SALVAT M and SUDO S (1980) Plasma Physics 22, 289-302.

BAUMHACKER H, BRINKSCHULTE H, BUCHL K, HASHMI M, MARLIER S F, RIEDMULLER W and SALVAT M (1977), 8th Eur. Conf. on Controlled Fusion and Plasma Physics, Prague 1977 (Czech Acad. Sciences) p.133.

BOLTON R A E, HUGILL J, LEES D J, MILLAR W, and REYNOLDS P (1971) 'Plasma Physics and Controlled Nucl. Fus. Research, Madison, USA, 1971', Vol. III, 79-92.

CROW J E, AUER P L and ALLEN J E (1975), J. Plasma Phys. 14, 65-76.

DAWSON J M (1964), Phys. Fluids 7, 981-987.

GATENBY P V and WALKER A C (1979) Culham Report CLM-R192 (Culham Laboratory, Abingdon, UK).

HAUGHT A F, POLK D H and FADER W J (1969), 'Plasma Phys. and Controlled Nucl. Fus. Research, Novosibirsk 1968' (IAEA Vienna) Vol. I, 925.

HAUGHT A F, POLK D H and FADER W J (1970), Phys. Fluids 13, 2842-2857.

HAUGHT A F et al (1978), United Technologies Research Center (USA) Report R78-954265-29 (COO-2277-12).

KITZUNEZAKI A, MITSUMORI T and SEKIGUCHI T (1974), Phys. Fluids 17, 1895-1902.

KLER C (1980), private communication.

KOGOSHI S, SPALDING I J, WALKER A C and WARD S (1980), J. Phys. E: Sci. Instrum. 13, 1170-1176.

LEES D J (1974), Culham Report CLM-R135 (Culham Laboratory, Abingdon, UK).

LINLOR W I (1964), Phys. Rev. Letts. 12, 383-385.

LUBIN M J, DUNN H S and FRIEDMAN W (1969) 'Plasma Phys. and Controlled Nucl. Fus. Research, Novosibirsk 1968' (IAEA Vienna), Vol. I, 945.

MCCRACKEN G M and STOTT P E (1979), Nuclear Fusion 19, 889-898.

PECHACEK R E, GREIG J R, RALEIGH M, KOOPMAN D W and DESILVA A W (1980), NRL Memorandum Report 4162, Naval Research Laboratory, Washington DC.

PFIRSCH D and SCHLUTER A (1962) Max Planck Institute (Garching, Munich) Report MPI/PA/7/62.

REYNOLDS P R, MILLWARD P, HUNT R R (1975) 'Plasma Physics and Controlled Nuclear Fusion Research, Tokyo 1974' (IAEA Vienna), Vol. II, 13.

REYNOLDS D A, STAMATAKIS T and WALKER A C (1980), Proc. 4th National Quantum Electronics Conf., Edinburgh 1979 (J Wiley & Sons, London) Paper 14.

SPALDING I J, ARMANDILLO E, DONALDSON T P, KACHEN G I, WALKER A C and WARD S (1977) 'Plasma Physics and Controlled Nuclear Fusion Research Berchtesgaden FRG 1976' (IAEA Vienna), Vol II, 589.

SUCOV E W, PACK J L, PHELPS A V, ENGELHARDT A G (1966) Westinghouse Research Labs. (USA) Report 66-1EO-PLASL-R2.

WALKER A C, STAMATAKIS T, SPALDING I J (1978a) J. Phys. D: Appl. Phys. 11, 2285-2293.

WALKER A C, KOGOSHI S, STAMATAKIS T and SPALDING I J (1978b) Optics Commun 27, 247-252.

APPENDIX

Incomplete pellet ionization is unlikely to be the major source of the neutrals involved in the charge-exchange energy loss for the following reasons:

(i) During initial generation of the laser-plasma, neutral material evolving from the rear of the irradiated pellet will be ionized by the surrounding corona. This plasma, which is maintained by electron thermal conduction, envelops the pellet (see Figure 5a) and has a temperature of at least 10 eV in this region. Taking the ionization rate for deuterium atoms when T_e = 10 eV to be $\langle\sigma v\rangle = 4 \times 10^{-15}$ m^3 sec^{-1}, the ionization time constant at a coronal density of 10^{23} m^{-3} is only 2.5 ns. The competing process of charge exchange could produce neutrals moving as fast as 10^5 m sec^{-1} but the consequent ionization distance of $\sim$ 40 μm (allowing for the 6 times greater ionization cross-section of the more energetic particle) is short compared with the density scale length of > 1mm. Since the laser irradiation continues until full pellet ablation is completed it would appear difficult for a significant density of neutrals to be generated. It can readily be shown that three-body recombination of the expanding coronal plasma from its measured initial condition (T_e = 100 $\sim$ 200 eV, $n_e = 10^{25}$ m^{-3}) should be insignificant.

(ii) During the first $\sim$ 1 ms of the confinement phase (when a large fraction of the energetic ions are lost via charge-exchange) the electron temperature is > 10 eV and the density $\sim 10^{19}$ m^{-3}. These values give an ionization time of $\leq$ 25 μs, which is also short compared with the 0.5-1.0 ms duration of the observed $\sim 2 \times 10^{16}$ m^{-3} average neutral density. It must therefore be concluded that there is a continuous source of neutrals during this period, i.e. material is desorbed from the torus walls by the escaping plasma.

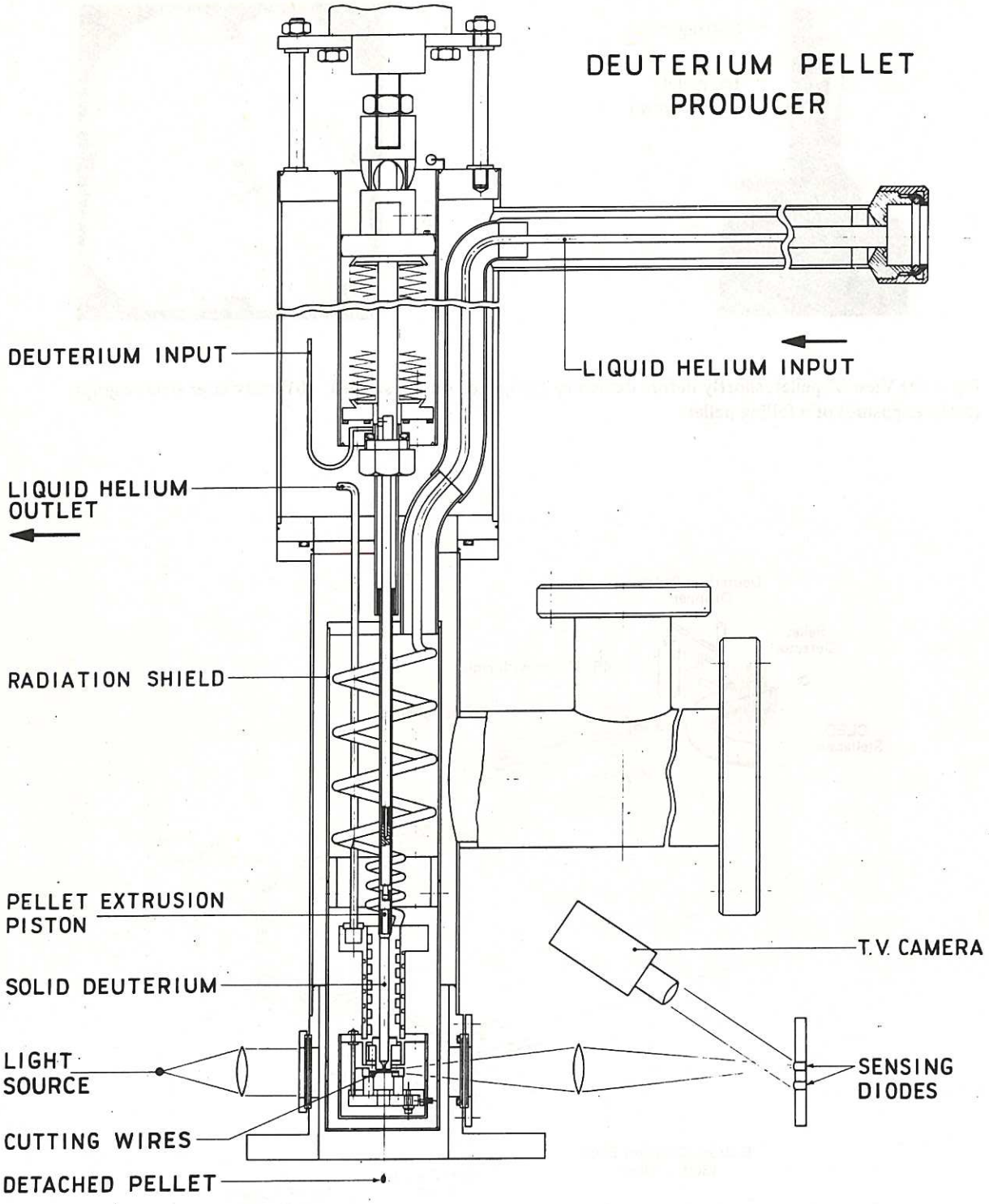

Fig.1 General diagram of the Leybold-Heraeus deuterium pellet dropper.

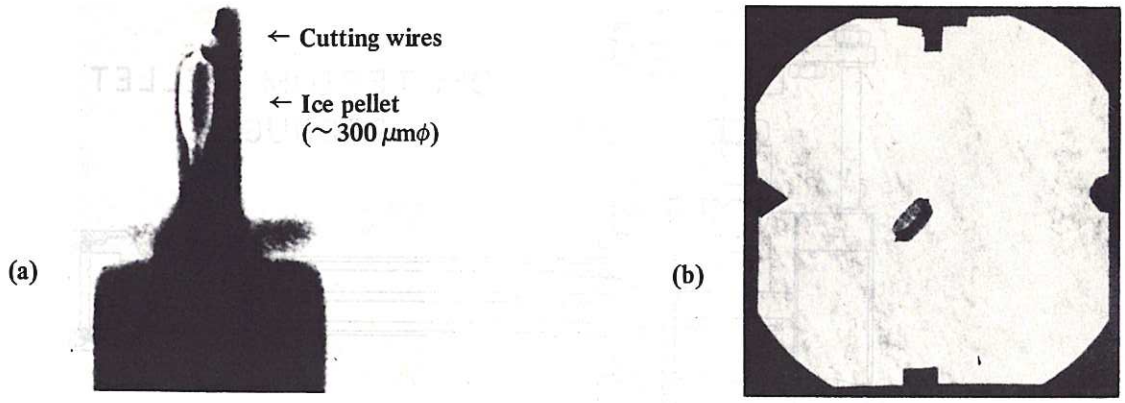

Fig.2 (a) View of pellet, shortly before detaching (projected onto a screen); (b) Ruby laser shadowgraph (50 ns exposure) of a falling pellet.

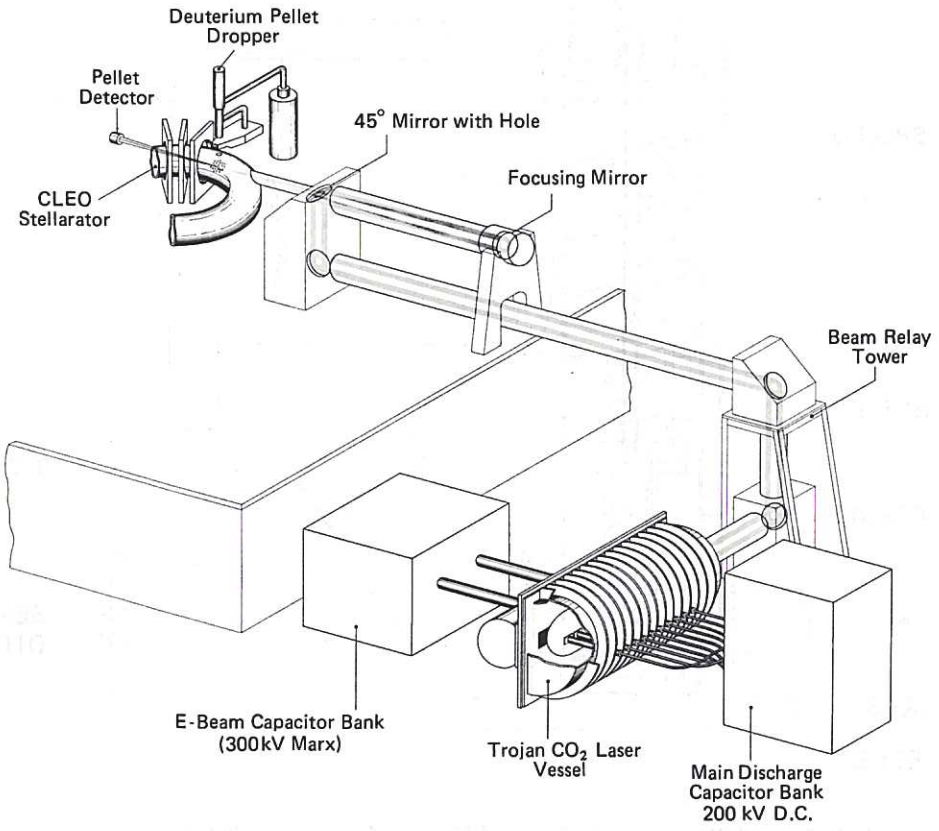

Fig.3 Diagram of the overall layout: showing TROJAN CO_2 laser, CLEO stellarator and the connecting optics.

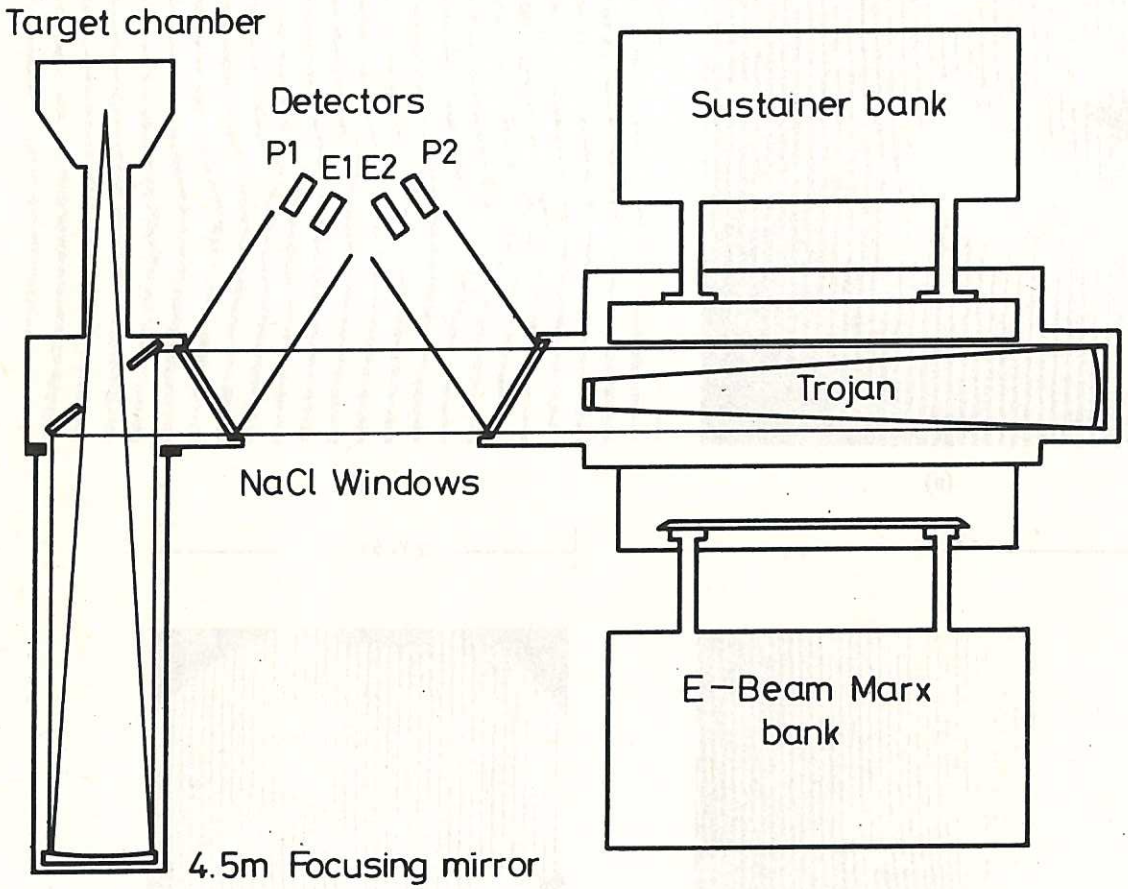

Fig.4 Plan-view diagram of TROJAN CO_2 laser, focusing optics and test target chamber.

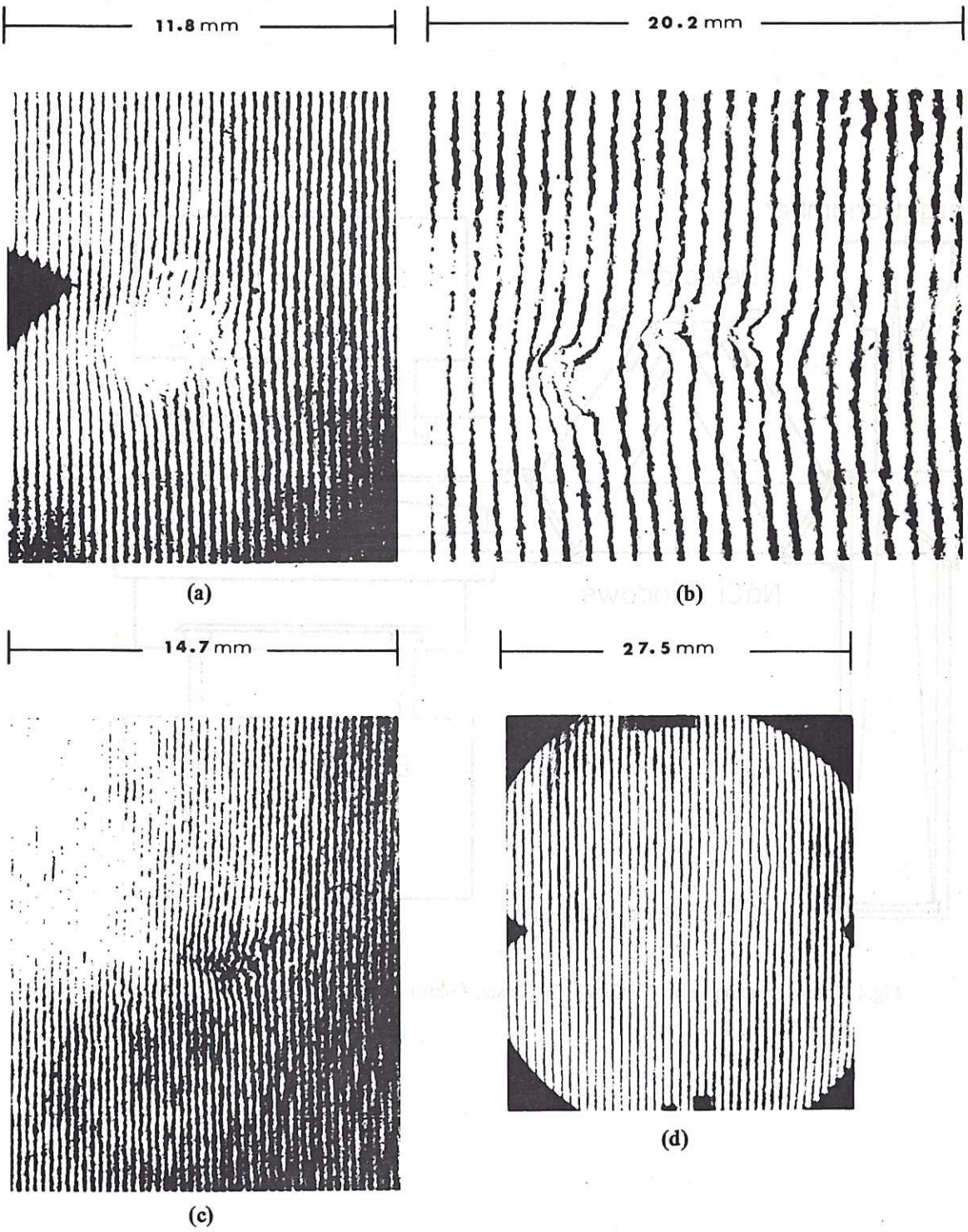

Fig.5 Interferograms of D_2 plasma: (a) 0·7 μs, (b) 1·2 μs, (c) 1·7 μs, (d) 2·8 μs from start of TROJAN pulse (CO_2 laser incident from left). Fringe shifts to the left correspond to increasing electron density.

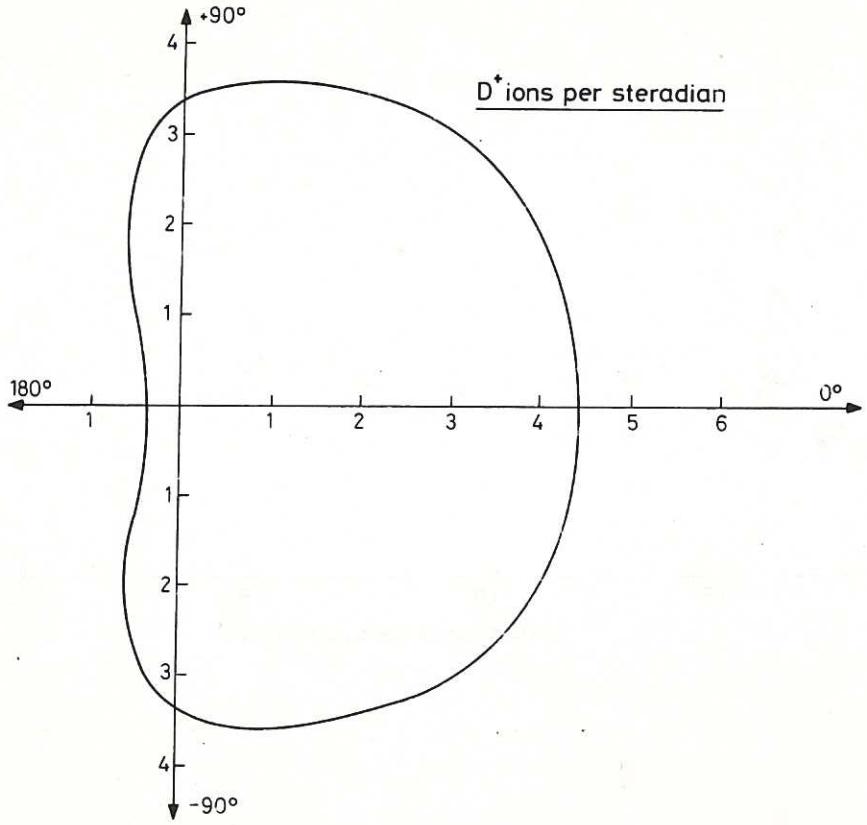

(a)

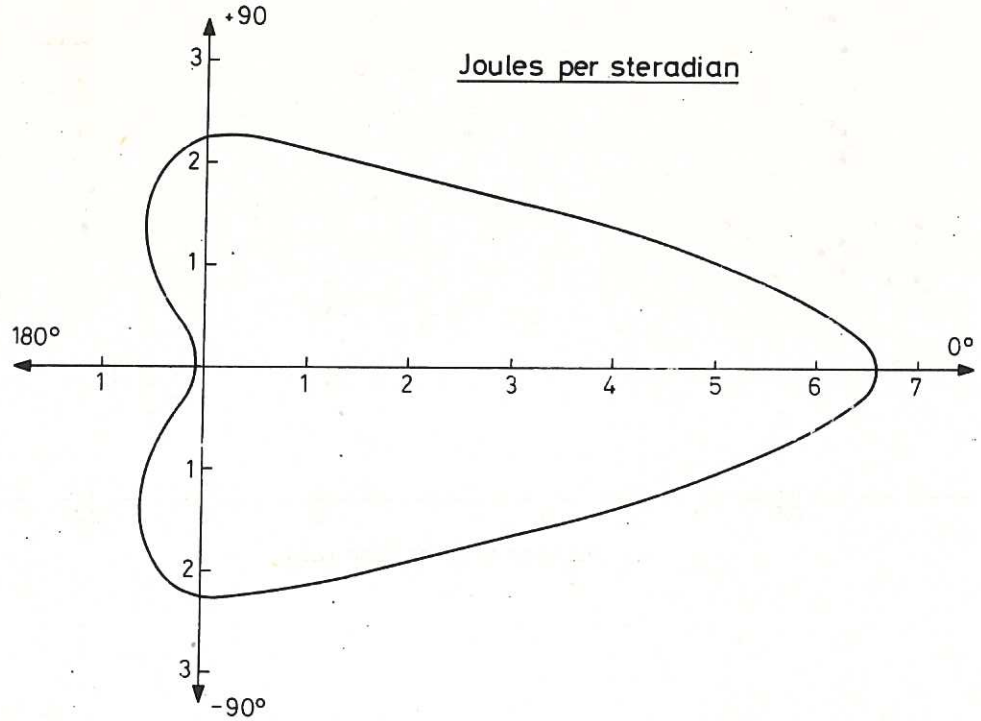

(b)

Fig.6 Distribution of (a) ions and (b) energy within the expanding laser-generated plasma, as determined by Faraday-cup charge collectors, averaged over 16, ~ 1·4kJ shots. (O° lies towards the laser).

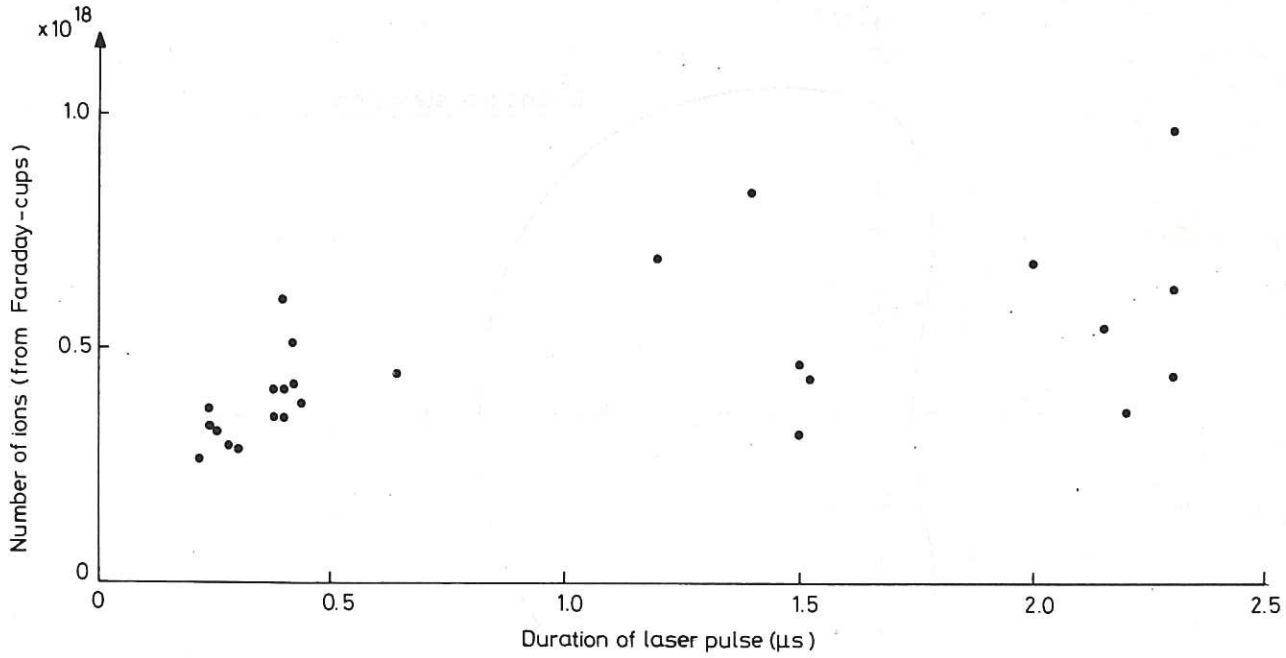

(a)

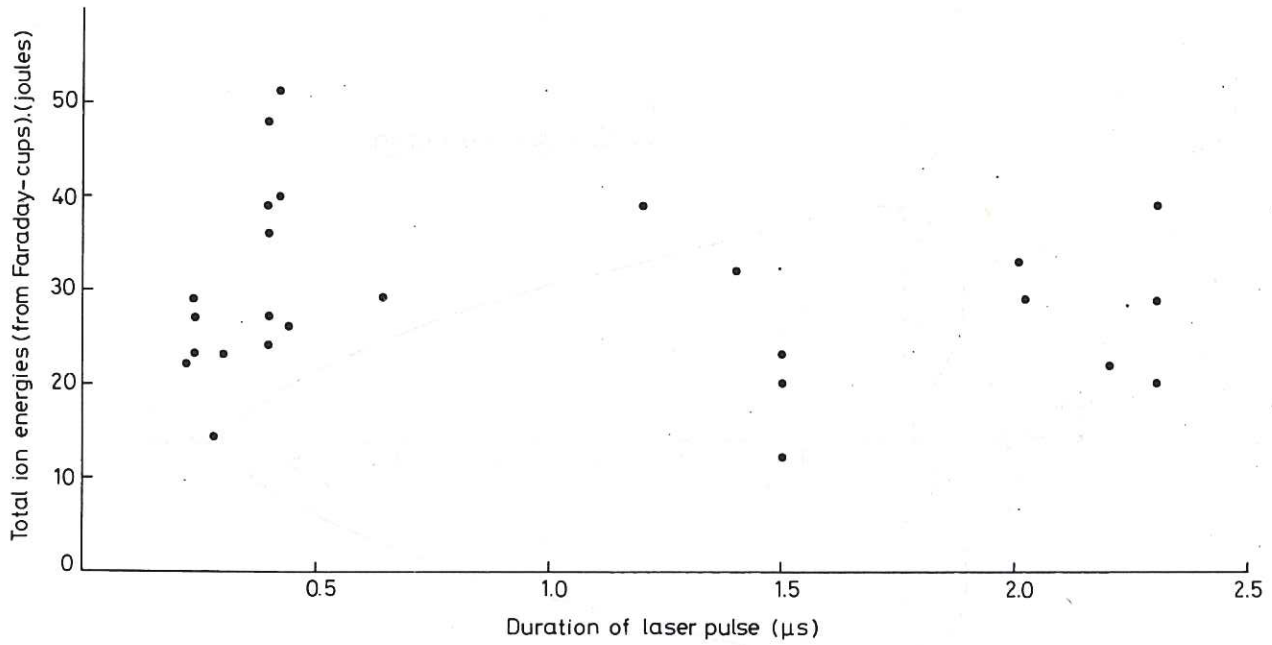

(b)

Fig.7 Variation of (a) total ion number and (b) the total energy they carry, with increasing laser pulse duration – deduced from (Faraday-cup) distributions of the type shown in Fig.6. (Incident energy for the shortest pulses: ~ 450 J and for the longest pulses: ~ 1·5 kJ.)

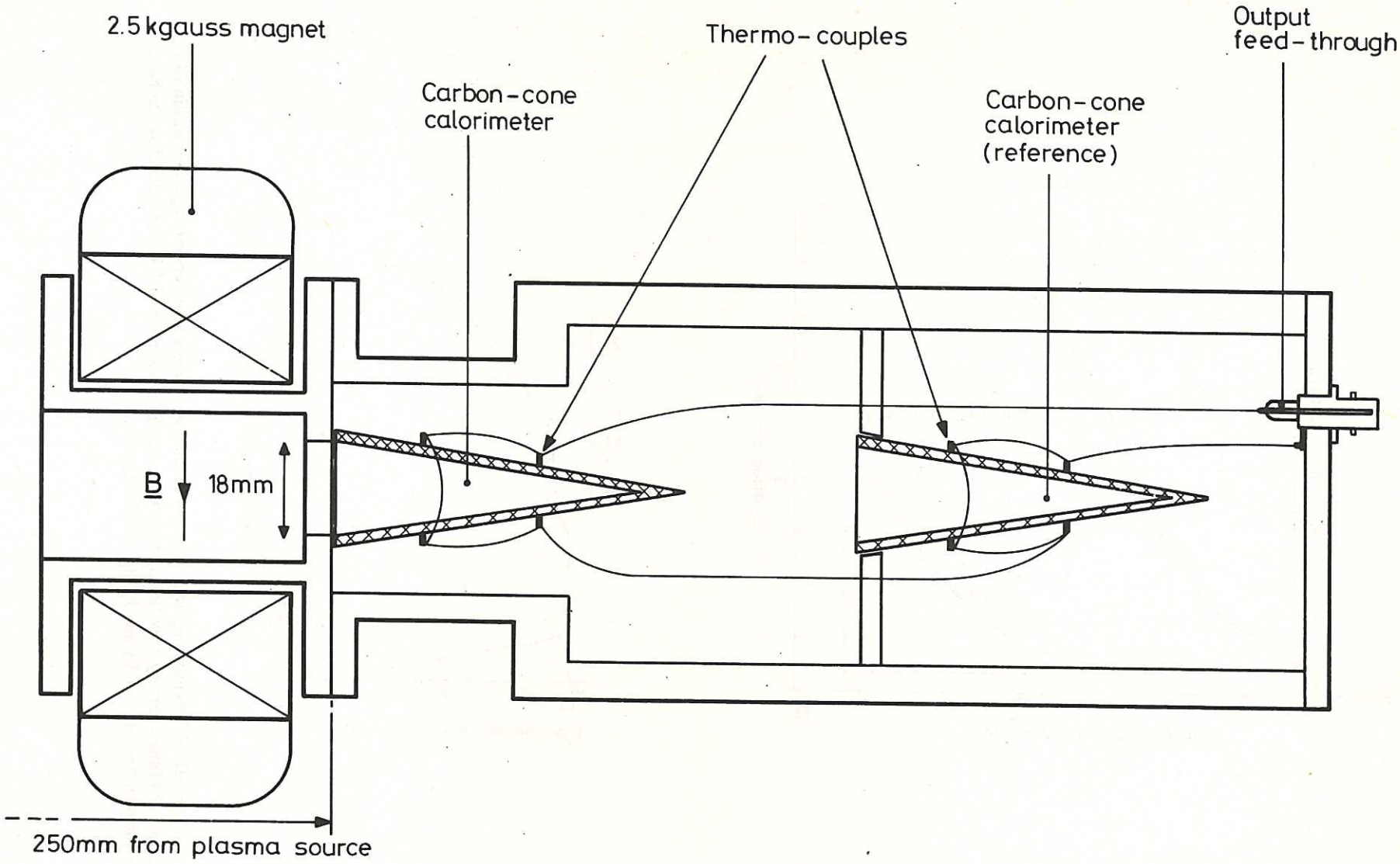

Fig.8 Diagram of calorimeter with deflection magnet in place.

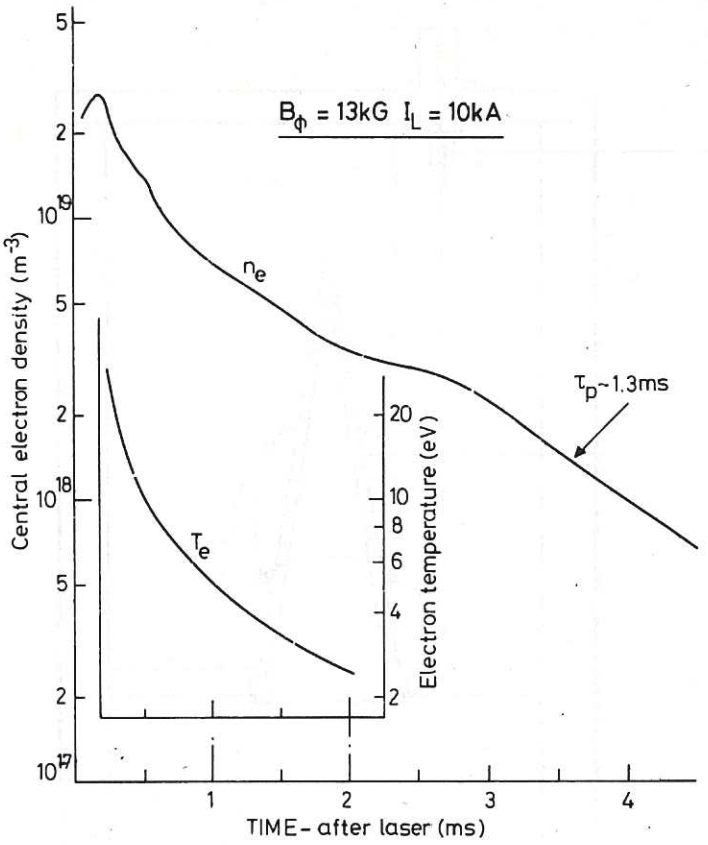

(a)

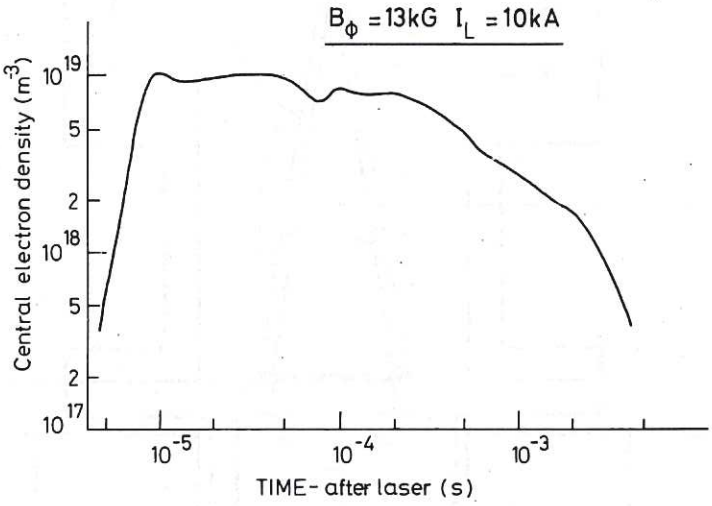

(b)

Fig.9 (a) Typical (high density) n_e and T_e versus time curves for the laser-generated plasma within CLEO stellarator. (b) Initial density peak (logarithmic time scale) for a similar TROJAN/CLEO shot. In both cases: toroidal field B_ϕ = 1·3 T and $I_L/B_\phi \sim$ 0·8 kA/kG.

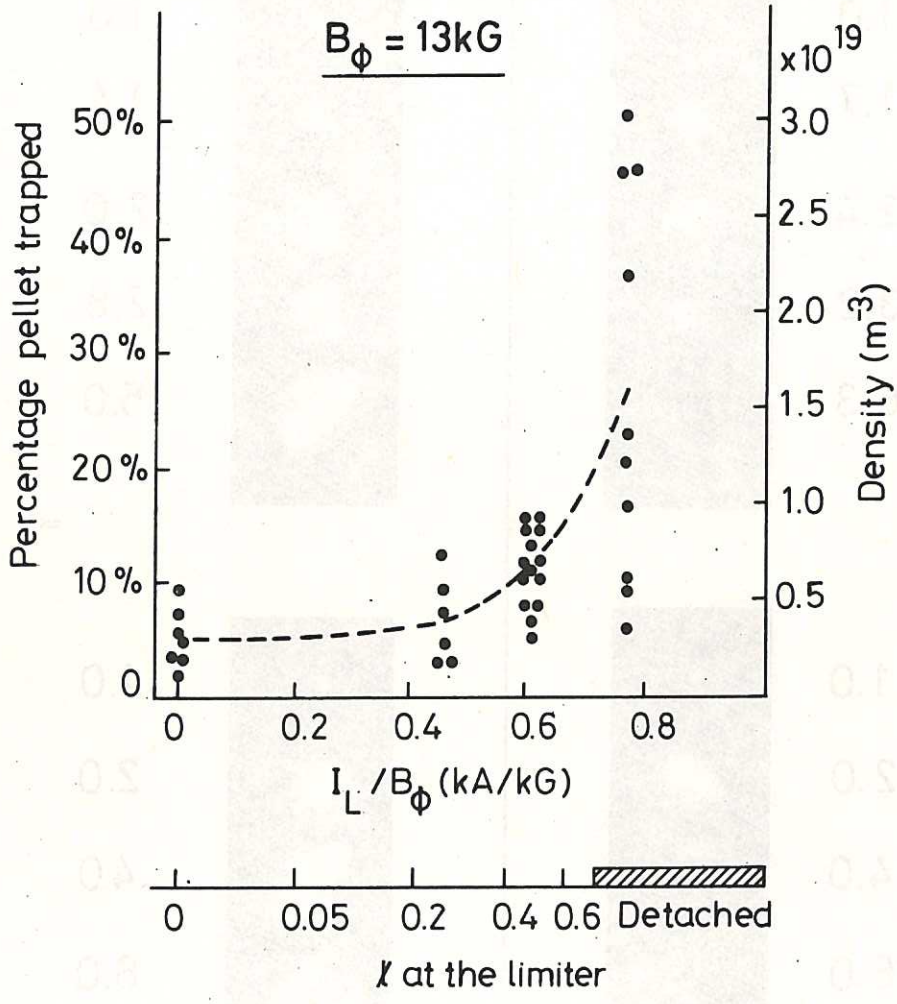

Fig.10 Peak density (percentage of pellet trapped) as a function of the ratio of helical winding current to toroidal field (i.e. rotational transform). Above $I_L/B_\phi \sim 0{\cdot}7$ the separatrix lines within the limiter radius. Each point represents a single TROJAN/CLEO shot except at $I_L/B_\phi = 0$ where each represents the average of four similar shots. Dotted line indicates average trend.

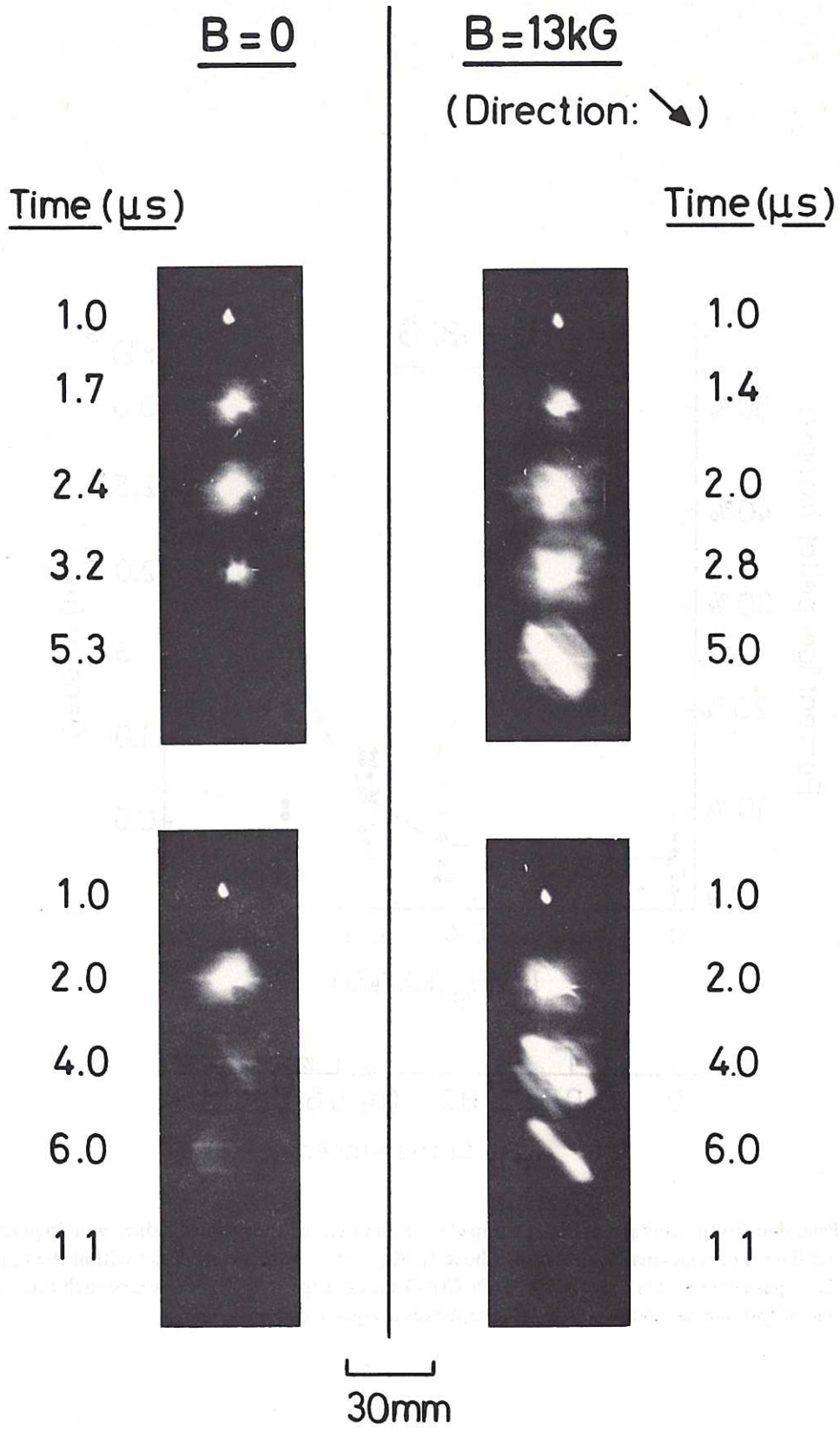

Fig.11 Framing camera photographs of expanding laser-generated plasma inside CLEO stellarator with and without the toroidal field (I_L = 0). Time is measured from the start of the laser pulse.